Surface Atmospheric Conditions Associated with Arctic Sea Ice Retreat, Resolved by the Arctic System Reanalysis

Undergraduate Research Thesis

Presented in partial fulfillment of the requirements

For graduation with *Honors Research Distinction in Earth Sciences*

In the undergraduate colleges at The Ohio State University

By

Stephen Bernard Maldonado

The Ohio State University

2017

Approved by

David H. Bromwich, Advisor
Department of Geography

W. Berry Lyons, Advisor
School of Earth Sciences

TABLE OF CONTENTS

Abstract

The years 2007 and 2012 witnessed two of the lowest levels of Arctic sea-ice extent in recorded history. A key indicator of climate change on a global scale, sea-ice dynamics – and the processes behind them – is vital to understanding and predicting changes throughout the Earth System. In data-sparse regions such as the Arctic, reanalyses (syntheses made from a combination of atmospheric models and observed data) are increasingly utilized to understand regional processes better. Largely dependent on model structure, physical assumptions, and data assimilation techniques, reanalyses often vary in their output quality and estimates of the ice-ocean-atmosphere interactions. The Arctic System Reanalysis (ASR) provides a high resolution (15km horizontal spacing for version 2, ASRv2) and skillful depiction of Arctic atmospheric processes. With a goal of better understanding the consequences of sea-ice retreat in the Arctic, an analysis of monthly average surface atmospheric conditions and trends is presented, focusing on indicators of boundary layer processes such as surface temperature, precipitation, humidity, and near-surface radiative fluxes. To confirm the reliability of this analysis, comparisons of ASR to surface observations from various sources are also presented. Findings from the analysis suggest that atmospheric processes play a large role in sea-ice retreat, while also providing insight into the efficacy of reanalyses for understanding the Arctic system.

Acknowledgements

This research would not be possible without the gracious encouragement and support of many people. At The Ohio State University, I am indebted to my advisors Professors David H. Bromwich and W. Berry Lyons. Without their insight and investment in me, these accomplishments would have never been conceivable. Moreover, I am vastly thankful for Professor Alvaro Montenegro, who has encouraged me to work hard in my academic endeavors, while remembering to smile along the way. I am forever grateful for the guidance and support of Professor Anne Carey, who has helped me to complete my undergraduate journey in every step of the way. I am also grateful for the Honors Arts and Sciences Undergraduate Research Scholarship, which has helped to fund my education and research.

At the Byrd Polar and Climate Research Center, I would like to acknowledge Dr. Sheng-Hung Wang, whose guidance has helped me develop a proficiency in computer programming that I would have never thought possible. Furthermore, I would like to thank Professor Ellen Mosley-Thompson, whose commitment to teaching has inspired me never to give up when dealing with such universal issues as those coupled with the Anthropocene. I would also like to thank Dr. Aaron Wilson, Dr. Julien Nicolas, and the rest of the Polar Meteorology Group, who have collectively devoted much of their personal time to help me progress and learn.

In both my undergraduate majors, Earth System Science and Atmospheric Science, I have been exceedingly blessed from my interactions with so many passionate instructors and professors. Their dedication to research and teaching has inspired me throughout the years. I have taken many classes at Ohio State (over 170.5 credits worth, at the time this thesis was written), and I am proud to say that I have gained a unique perspective on life from every single instructor, teacher, and professor that I have interacted with over the past four and a half years.

My scientific passion would be nothing without the enthusiasm and inspiration of those with whom I was raised. I am immensely grateful for my preliminary education, as I would not have pursued a degree in the sciences if it weren't for the interest in science instilled by my K-12 teachers including Dr. Paul Brendel, Mr. Bob Spira, and Ms. Silva Michel.

Lastly, I would like to acknowledge my peers, friends, and family. To say I have been privileged in my academic career would be an immeasurable understatement, and I would not be where I am today without their encouragement and support. Words cannot express how thankful I am to have such very special people in my life.

List of Figures

List of Tables

Introduction

Sea ice is a vital element of the Arctic Ocean and the processes that govern its dynamics. It is a major control in exchanges of heat, gas, and water in the Arctic atmospheric boundary layer. Likewise, the retreat of sea ice is recognized as an unambiguous sign of a changing climate (Hassol, 2005). As measured from a variety of sources, Arctic sea ice has been declining at a sharp rate over the past few decades. Submarine draft measurements presented by Rothrock et al. (1999), Arctic sea ice has thinned by roughly 40% from the 1960s and 70s into the 1990s. Likewise, satellite observations from 1979–2006 have measured a rate of decline in September sea ice extent (climatological annual minimum) of about -9.1% per decade (Stroeve et al., 2007). The annual minimum of Arctic sea ice measured in September, 2012 was the lowest in the satellite era. Records were set as both the total cumulative area of sea ice and the areal extent of ocean containing at least 15% sea ice were the lowest measured in the more than three decades of satellite measurements (Parkinson and Comiso, 2013). Moreover, the previous sea ice extent record minimum set in 2007 (approximately 4.2 million km^2) was 23% less than the record minimum set before that, in 2005 (Stroeve et al., 2008). As such a critical component of the Arctic climate system, and as such a rapidly changing region on our planet, studying sea ice has proven to be an imperative aspect of forecasting potential future climates.

Although studying changes in the Arctic is so imperative, *in situ* measurements are often few and far between. To remedy this issue and to understand better the dynamics on a larger scale, atmospheric reanalyses have been widely utilized as a way of investigating atmospheric and boundary-layer processes in the Arctic. Thought of as a blending of observations and climate model physics, reanalyses offer an insight into the variability and trends in many atmospheric processes that would otherwise could not be studied.

While atmospheric reanalyses have been widely accepted as a useful tool for studying changes in the Arctic, their output is sometimes received with caution, as known uncertainties occasionally cast doubt on the insight gained from such blended observations and models. One such uncertainty deals with a reanalysis' output variables, and is explained well by Kalnay et al. (1996). In the literature, distinction is made to assess an output variable's reliability, with variables classified depending on the degree by which they are influenced by observations or the model. As an example, "Class A" variables are those that are strongly influenced by observations, and include variables such as surface temperature or sea level pressure. Likewise, "Class C" variables are those that are completely dependent on model physics, and include variables like surface radiative fluxes and precipitation. This thesis deals with such variables, and uncertainties in the model are noted as such.

Another uncertainty associated with atmospheric reanalyses deals with the gridded structure of the model, and how topography is smoothed. To understand, one can imagine a mountainous region consisting of peaks and valleys that is simplified by a reanalysis model. In such a hypothetical scenario, a gridded reanalysis model would generalize the topography as having a surface elevation that could be higher or lower than what exists in reality. If, for example, the "smoothed" topography were hundreds of meters higher than what exists at a station, the model would perform calculations for surface variables as conditions that exist hundreds of meters in the atmosphere. This effectively leaves out the lowest reaches of the atmospheric boundary layer, typically where the most moisture is found. This would influence cloud and precipitation producing processes and the radiative forcing from the lowest parts of the atmosphere. This discrepancy is touched upon later in this thesis, where ASR's model interpolation of height comes into account for various surface variables.

With uncertainties in model physics and the gridded structure that varies from case to case, reanalyses can have vastly different products. Lindsay et al. (2014) presented a comparison of different reanalysis models over the 30-year time period of 1981–2010. In this analysis, monthly

averaged surface temperatures, radiative fluxes, precipitation, and wind speed were compared to *in-situ* measurements to assess each reanalysis' ability to capture seasonal variability. Lindsay et al. (2014) found that three reanalysis models (Climate Forecast System Reanalysis or CFSR, Modern-Era Retrospective Analysis for Research and Applications or MERRA, and the ECMWF Interim Re-Analysis or ERA-Interim) performed significantly better than four other models, including the National Centers for Environmental Prediction (NCEP)-National Center for Atmospheric Research Reanalysis 1 (NCEP-R1) and NCEP-US Department of Energy Reanalysis 2 (NCEP-R2), the Twentieth-Century Reanalysis (20CR), and the Japanese 25-year Reanalysis Project (JRA-25). The Ohio State University's ASR was not included in this comparison as it was incomplete at the time work was being done by Lindsay et al. More recently, Chaudhuri and Ponte (2015) presented a preliminary ASRv1 (30km resolution as compared to ASRv2's 15km resolution). In the comparison, model outputs were compared to satellite-observed surface conditions that included such surface atmospheric variables compared in Lindsay et al. (2014) (2m temperature, surface radiative fluxes, 2m humidity, etc.). The analysis concluded that several of the reanalyses presented discrepancies from remote measurements, and highlighted errors in ASR's version 1 that were addressed in preparation for version 2 (such as inconsistencies in radiative fluxes and precipitation).

Later still, Kohnemann et al. (2017) presented an analysis of extreme changes in the Arctic in the region of the Kara and Barents Seas (identified in Figure 1). The analysis utilized two atmospheric reanalyses to investigate extreme changes in the Arctic from wintertime 2003/04 to wintertime 2014/15. The models used were: Consortium for Small-Scale Modeling (COSMO) in Climate Limited-Area Mode (CCLM) and ASR Version 1. The analysis presented high spatial and temporal variability of 2m temperature increases in the Arctic, highlighted by a maximum temperature increase of about 20°C between March 2003 and 2012. Additionally, 2m temperature increases in the Arctic during the first decade of the 21st century was shown to be up to eight times

greater than in decades before. Such drastic changes raised alarms for the Arctic research community and have been interpreted as a climate regime shift in the area, especially during the month of March as sea ice cover has become substantially reduced.

Recent literature illuminating extreme changes in the Arctic using atmospheric reanalyses have both highlighted the efficacy of atmospheric reanalyses for their ability to precisely capture variability and trends in the Arctic, and the need to investigate the processes behind the perceived "tilting points" associated with 21st century climate change. Moreover, existing literature that compares various reanalysis products that exclude the current version of the Arctic System Reanalysis has left a void that can be improved by the research presented in this thesis.

DATA AND METHODS

Data Collection

Primary data for this research were collected from the publically available ASR Project from the Polar Meteorology Group of the Byrd Polar and Climate Research Center. Specifically, ASRv2 (15km resolution) data were downloaded from NCAR's Research Data Archive (RDA). Observation data records for this research were collected from two sources: for precipitation, temperature, specific humidity, and pressure records, data from ~30 meteorological stations were downloaded from the Global Historical Climatology Network (GHCN) found publically through the National Oceanographic and Atmospheric Administration's (NOAA) National Centers for Environmental Information (NCEI) online database. Radiation data for ~10 meteorological stations were collected from the Baseline Surface Radiation Network (BSRN) of the World Radiation Monitoring Center (WRMC).

Arctic System Reanalysis

The ASRv2 is a 15km resolution reanalysis of the Arctic produced by the Polar Meteorology Group at Ohio State University's Byrd Polar and Climate Research Center. The output includes more than 100 atmospheric variables for 29 vertical levels over the time period 2000–2012 and is available at NCAR's Research Data Archive (RDA). A full description of the Arctic System Reanalysis Version 2 and its applications can be found in Bromwich et al. (2017). For comparison to weather stations of other variables, ASRv2's gridded structure was interpolated to given latitude/longitude coordinates using scripts written in NCAR Command Language (NCL) utilizing a bilinear interpolation. Regressions were then performed over the 2000–2012 time period using NCL's regression functions.

Radiation Analysis

For analysis of data from the BSRN, data were originally formatted in 1 and 5 minute increments in ASCII format. To process these data, files were converted to a space-delimited text format using the "BSRN Toolbox" available for download on the WRMC website. After processing the files into a space delimited text format using the BSRN toolbox, the files were then broken down by column into variables stored in netCDF format. This process was completed using a script written for NCL. During this conversion process, data were averaged at increments of every three hours (±30 minutes). The above scripts are included in Appendices A through C.

Temperature/Precipitation Analysis

For temperature and precipitation records collected through the GHCN, data were processed using NCL. GHCN data were available in an adjusted and unadjusted format. According to NOAA's NCEI, various statistical methods are performed on the raw data to improve accuracy, however adjusted data were not available for every station. When available, the adjusted data were preferred and used. In stations that did not have a record of adjusted data, unadjusted data were used for calculations, and these stations are marked accordingly. Monthly averaged GHCN files were initially downloaded and processed into text files, where individual analyses were performed on a station by station basis. To do so, station metadata (from GHCN) were saved as variables in a shell script and then read into an NCL script that read the tab delimited text files and reformatted data into netCDF files. In this NCL script, UTC time coordinates were assigned to each netCDF file to make regressions easier. These scripts are included in Appendix D. Long term regressions were performed on stations and compared to output by ASR using the same bilinear interpolation and regression method as discussed above. A sample NCL script for these interpolations and regression calculations is included in Appendix E.

RESULTS

Arctic System Reanalysis

In the region that encompasses most of the ASR domain, locations of stations for which *in situ* observations were compared with ASR are highlighted (Figure 1). In addition, locations (such as the Kara and Barents Seas, the island of Novaya Zemlya, and major continents) are shown in italics for reference.

The region of Novaya Zemlya and the Kara and Barents Seas are of particular interest because of their drastically changing climate, as evidenced in Figure 2, which shows linear trends in sea ice fraction for the month of January, over the time period of 2000–2012, from the ASR. Figure 2 illustrates the most statistically significant trends for the region near Novaya Zemlya, where sea ice fraction has reduced by roughly 4% per year from 2000–2012, amounting to an approximate 50% reduction in sea ice (in some locations) during the month of January. Moreover, similar trends were produced by ASR in 2m temperature, specific humidity, downward longwave radiation, and precipitation. Figure 3 illustrates those trends, which show increases in temperature of approximately 1°C yr^{-1} (~13 °C from 2000–2012), increases in specific humidity of ~0.12 g $kg^{-1}yr^{-1}$ (~1.50 g kg^{-1} from 2000-2012), increases in longwave radiation around 5 Wm^{-2} yr^{-1} (~60 Wm^{-2} from 2000-2012), and increases in precipitation of about 10 % yr^{-1} (over 100% increase from 2000–2012).

These trends are consistent with those presented in Kohnemann et al. (2017) that highlight the effect of reduced winter time sea ice extent on increased sea-to-atmosphere heat and moisture flux. As is discussed in the literature, open water supplies water vapor and heat to the atmosphere. This additional moisture contributes to an increase in downward longwave radiation as additional clouds and precipitation develop, that drives further increases in surface temperature and sea ice melt. It is notable, however, that significant positive precipitation trends are emphasized to the east

of the island of Novaya Zemlya. This translation is explained as moisture advection downwind of its source, and is consistent with mean 700mb flow (Figure 4).

Because of such dramatic trends, further validation was desired for additional insight into ASR's output. In particular, validations were sought for the forecast variables of longwave radiation and precipitation (classified as "Class C" variables). For this validation, *in situ* records were collected from the Global Historical Climatological Network (for analysis of precipitation records) and the Baseline Surface Radiation Network (for downward longwave radiation). Roughly 20 GHCN stations were analyzed for long term trends (for the time period in which records were available) as well as short term trends (for ASR's time period of 2000-2012). Likewise, about 10 BSRN stations were analyzed using a similar method.

Global Historical Climatological Network

The correlation of ASR's forecasts for precipitation and temperature compared to *in situ* records varied significantly among the many stations, however it is known that local topography is strongly responsible for discrepancies in measured precipitation. For the best representation of ASR's 15km x 15km grid structure, weather stations were selected with local topography in mind. Most desirable stations were those in flat, open terrain. Likewise, observations in the Arctic are known to be similarly uncertain because of the difficulty in accurately measuring the amount of frozen precipitation. With that in mind, preference was also given to stations at latitudes near or lower than the Arctic Circle (locations of these stations are shown in red in Figure 1). Results from the analysis of 9 "validating" stations are shown in Figure 5, showing linear regressions for the average January total precipitation for a range of years (varying by station) that encompass ASR's time domain. Comparative statistics (bias, root mean square error, and linear correlation) were calculated for each station (Table 1). As expected, sites with most ideal topography showed the

highest correlations when compared to ASR; five of nine "validation" sites exhibited linear correlations greater than 0.90, with an additional two sites exhibiting linear correlations greater than 0.80. The lowest correlation of the validation sites (0.64), calculated from the precipitation record at The Pas in Manitoba, Canada, only appears to be significantly lower than others because of missing data during the time period of 2000–2012. To supplement, the procedure was performed for temperature records also collected from the GHCN. Linear regressions and comparative statistics were calculated for nine "validation" sites. Results are displayed in Figures 7 and are summarized in Table 2, following the same pattern as in Figure 5 and Table 1. Extremely high correlations (all but four of thirteen stations had correlations greater than 0.95, with all stations above 0.90) attest to the general agreement between ASR and the records collected from the GHCN.

ASR's strong correlation to weather station records and ability to capture variability permitted further analysis of stations in the Arctic Ocean, specifically the region of interest near the island of Novaya Zemlya and surrounding seas. Results for the analysis of four more stations (all within the Arctic Circle and with non-ideal local topography) are shown in Figure 6 which also show linear regressions for average January total precipitation for long term (observation record) and short term (ASR domain) measurements. Comparisons to ASR are also summarized in Table 1. The temperature records from these stations are shown in Figure 8, with comparative statistics summarized in Table 2. Results from these stations show that ASR is capable of capturing variability to a good degree, with major discrepancies being explained by complex terrain and un-favorable conditions. For example, bias in the precipitation record at the Svalbard station may be explained by the difference in elevation that occurred from ASR's topography smoothing (Table 3). Likewise, topography smoothing may also be responsible for the temperature bias at the Tromsø station and the radiation bias at the Ny-Alesund station.

With the exception of Tromsø, all stations show an increasing trend in January precipitation, which is consistent with the assessment predicted from the ASR analysis, that reduced sea ice allows for increased sea-atmosphere moisture flux that mostly falls as precipitation. Notable, however, is the small temperature bias between the Tromsø station and ASR (-3.84 °C) that does not appear as significant in the precipitation record.

Baseline Surface Radiation Network

To validate radiation measurements, BSRN data were downloaded for 11 stations. The limitations in accuracy that exist for precipitation measurements do not apply as directly for radiation measurements. Because of this, combined with the fact that only a limited number of global stations accurately measure and publish radiation data meant that relevant stations were inherently low in number. Records for additional stations (Barrow, Alaska; Tiksi, Russia; Alert, Canada; and Eureka, Canada) were also available, but their data were excluded for various reasons (ie. Barrow's data were recalled from the BSRN by the managing researchers; Tiksi's record was not long enough to perform any significant comparison to ASR, etc.) The radiation record for only one station, Ny-Alesund on Svalbard Island, is shown in Figure 9, which shows ASR's ability to capture variability in a quantity produced mostly by model physics (as opposed to user input). The discrepancy in magnitude, however, is most likely explained by ASR's tendency to smooth over topography. In regions with varying topography, ASR can inadvertently assume a higher elevation at an interpolated point than is the actual the elevation at the radiometer station. Additionally, complex topography around the measurement station plays an important role in cloud formation and, therefore, the amount of longwave radiation emitted by the atmosphere down to the Earth surface. The trend shown in Ny-Alesund's record (and ASR's forecast) corresponds well in the larger context of Figure 3c, which shows downward longwave radiation trends produced by ASRv2.

Conclusions

Significant trends in the region of Novaya Zemlaya and the surrounding Kara and Barents Seas are consistent with those presented in Kohnemann et al. (2017), albeit to a slightly lesser magnitude. Positive trends in 2m temperature as presented by ASRv2 are demonstrated to be roughly 1.2 °C yr^{-1} (or approximately 15°C over the 13-year time period). Significant positive trends in 2m specific humidity, precipitation, and longwave radiation suggest that reduced sea ice cover is contributing to an enhanced sea-atmosphere heat and moisture flux in the region.

This analysis also suggests that ASRv2 is capable of capturing trends and variability with precise skill. High correlations calculated between *in-situ* records and ASR's output specifically of "Class C" variables like surface radiation and precipitation demonstrate ASR's versatility and efficacy as a tool for studying rapid changes in the Arctic.

Biases between ASR's output and observed records may be explained in several ways:

- ASR's overestimate of precipitation at the Svalbard station may be explained by the difference in elevation from ASR's topography smoothing, or could be a result of frozen precipitation being under-measured by an *in-situ* precipitation gauge.
- ASR's underestimate of 2m temperature at the Tromsø station may be explained by topography smoothing, as the ~4 °C difference could be reasonable considering a ~700m difference in elevation predicted by the model.
- ASR's underestimate of downward longwave radiation at the Ny-Alesund station could be a result of topography smoothing, as downward longwave radiation is closely tied to cloud production and moisture content in the atmosphere, which is often underestimated with an inconsistency in elevation

Moreover, the outlier in the precipitation record at the Dixon Island Station (January 2001) is under question, as it is extremely unlikely for precipitation during one month to be on the order of ~4-5 times those of other years (as it is recorded, cumulative precipitation in January 2001 is around 220mm, while other months' cumulative precipitation is around 40–60mm).

Recommendations for Future Research

Opportunities to explore atmospheric conditions and their role in sea ice retreat are plentiful. In particular, one could investigate:

- Additional connections to cloud-producing processes in the Arctic, with an emphasis on examining how cloud production is captured by the Arctic System Reanalysis, as well as other reanalyses
- The middle and upper atmospheric processes and their role in patterns observed at the surface
- Performing an elevation adjustment to ASR's output, considering each station's reported elevation
- Investigating patterns at seasonal and other intra-annual frequencies
- Connections to inter-annual patterns such as El-Niño Southern Oscillation, Madden-Julian Oscillation, or the North Atlantic Oscillation
- The role of oceanographic phenomena such as the Atlantic Meridional Overturning Circulation or the Gulf Stream in heat advection into the North Atlantic and Arctic Oceans

Areas of Interest

Figure 1: Locations of weather stations where data from the GHCN (Precipitation records, in red dots) and the BSRN (Longwave radiation records, in blue dots) are collected from. Notable locations/regions are shown in italics for reference. Precipitation stations marked with an asterisk used GHCN raw data, while precipitation stations without the asterisk used GHCN-adjusted data

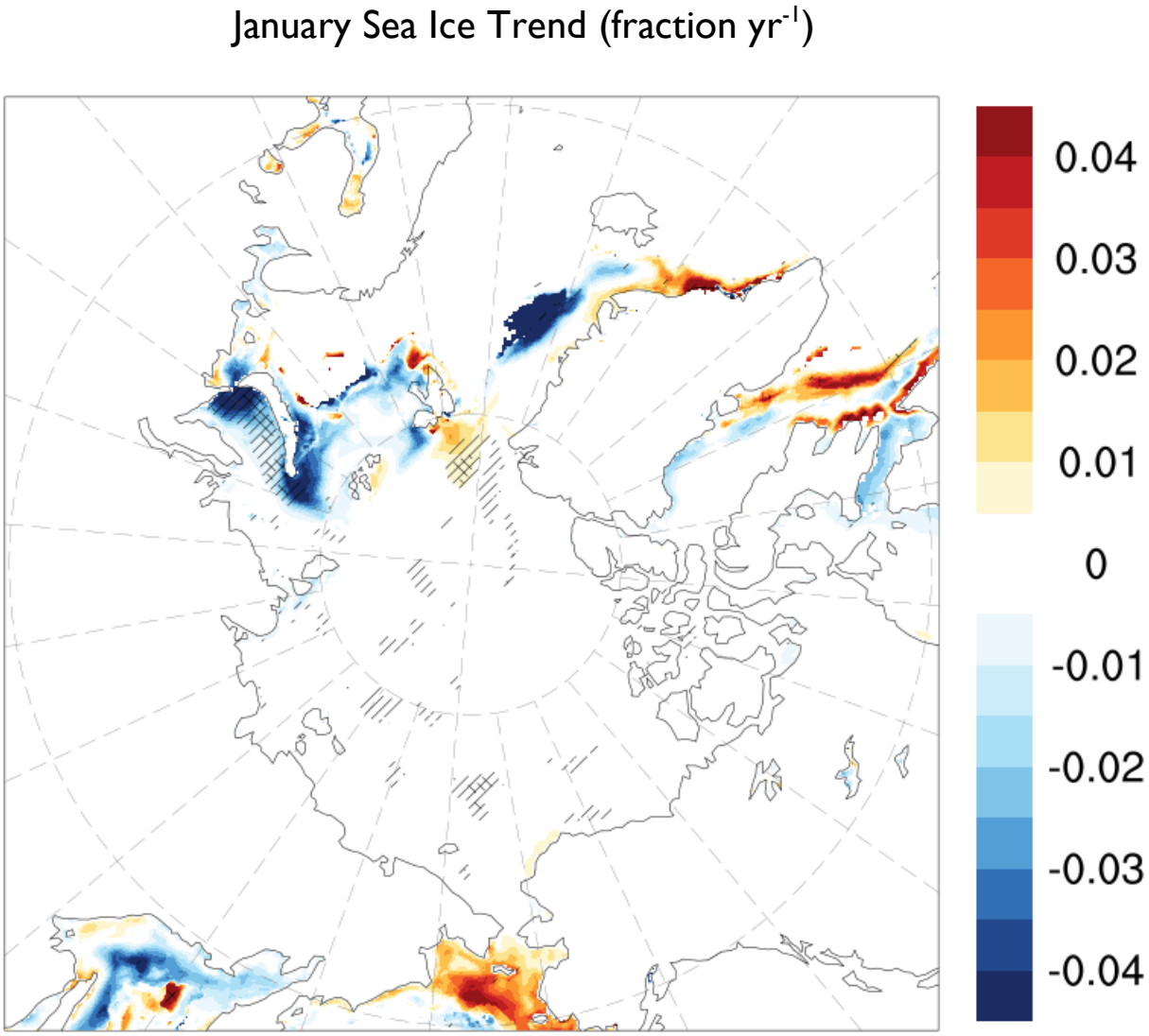

Figure 2: Linear January trends in sea ice fraction for 2000-2012 from ASRv2. Unidirectional hatch marks indicate p-values less than 0.05, while crossed hatch marks indicate p-values less than 0.01.

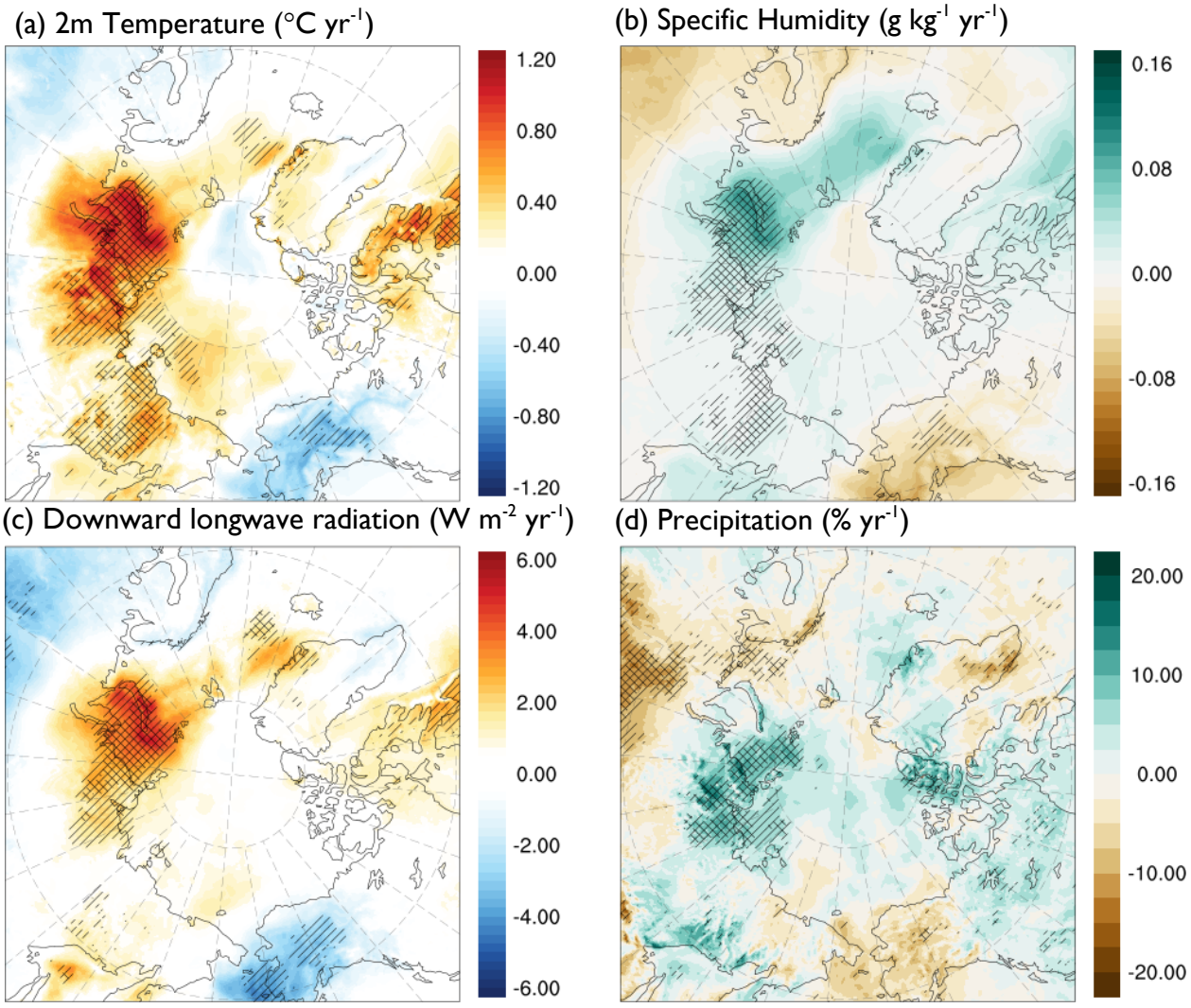

Figure 3: Linear trends in average January (a) 2m temperature, (b) specific humidity, (c) downward longwave radiation, and (d) monthly total percentage change in precipitation from ASRv2. Unidirectional hatch marks indicate p-values less than 0.05, while cross hatch-marks indicate p-values less than 0.01.

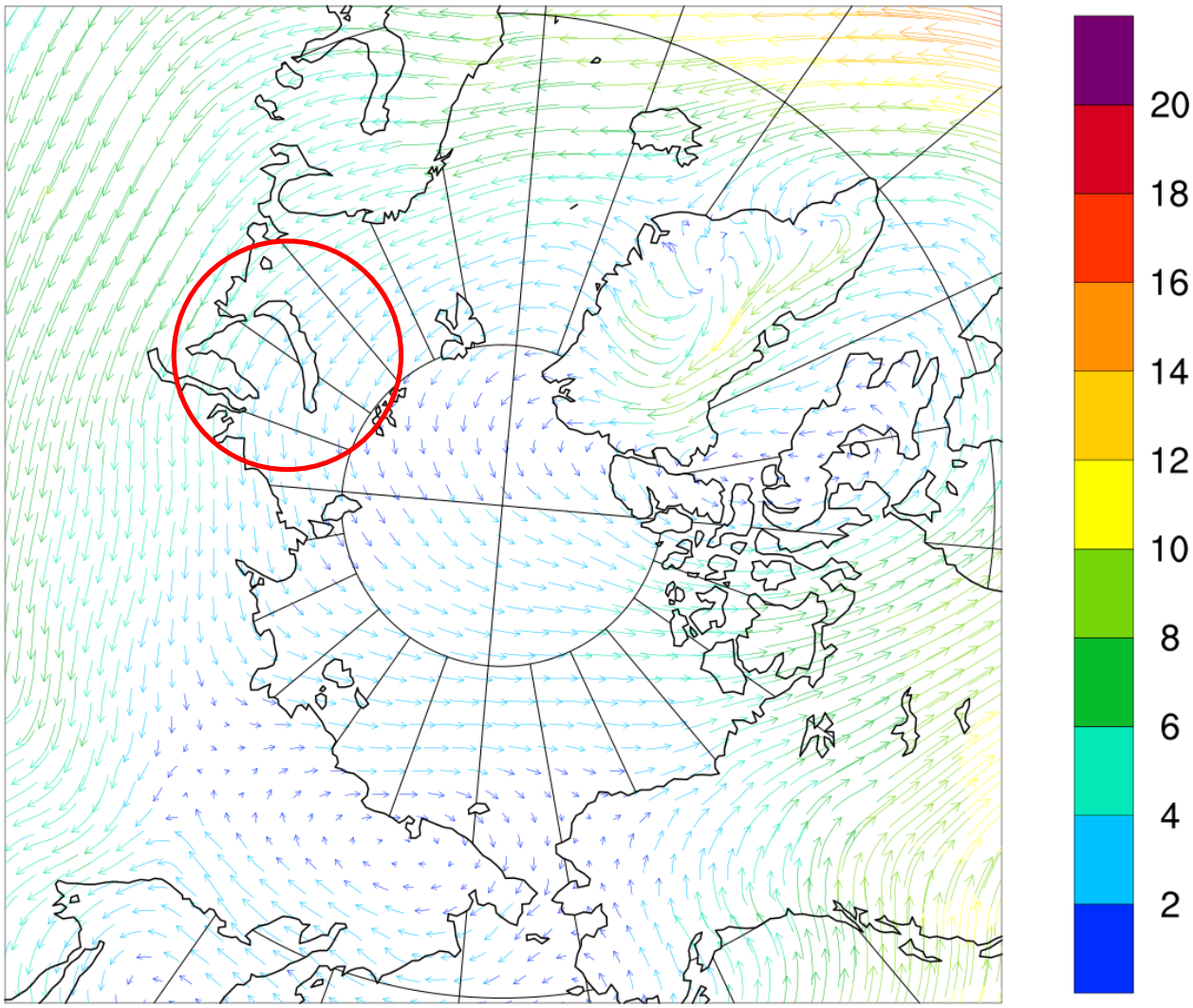

Figure 4: January vector averaged wind speed over the time period of 2000–2012 at the 700mb level (in m s^{-1}) for comparison of precipitation trends shown in Figure 3. Highlighted are eastward winds over the island of Novaya Zemlya that carry moisture downwind of the island.

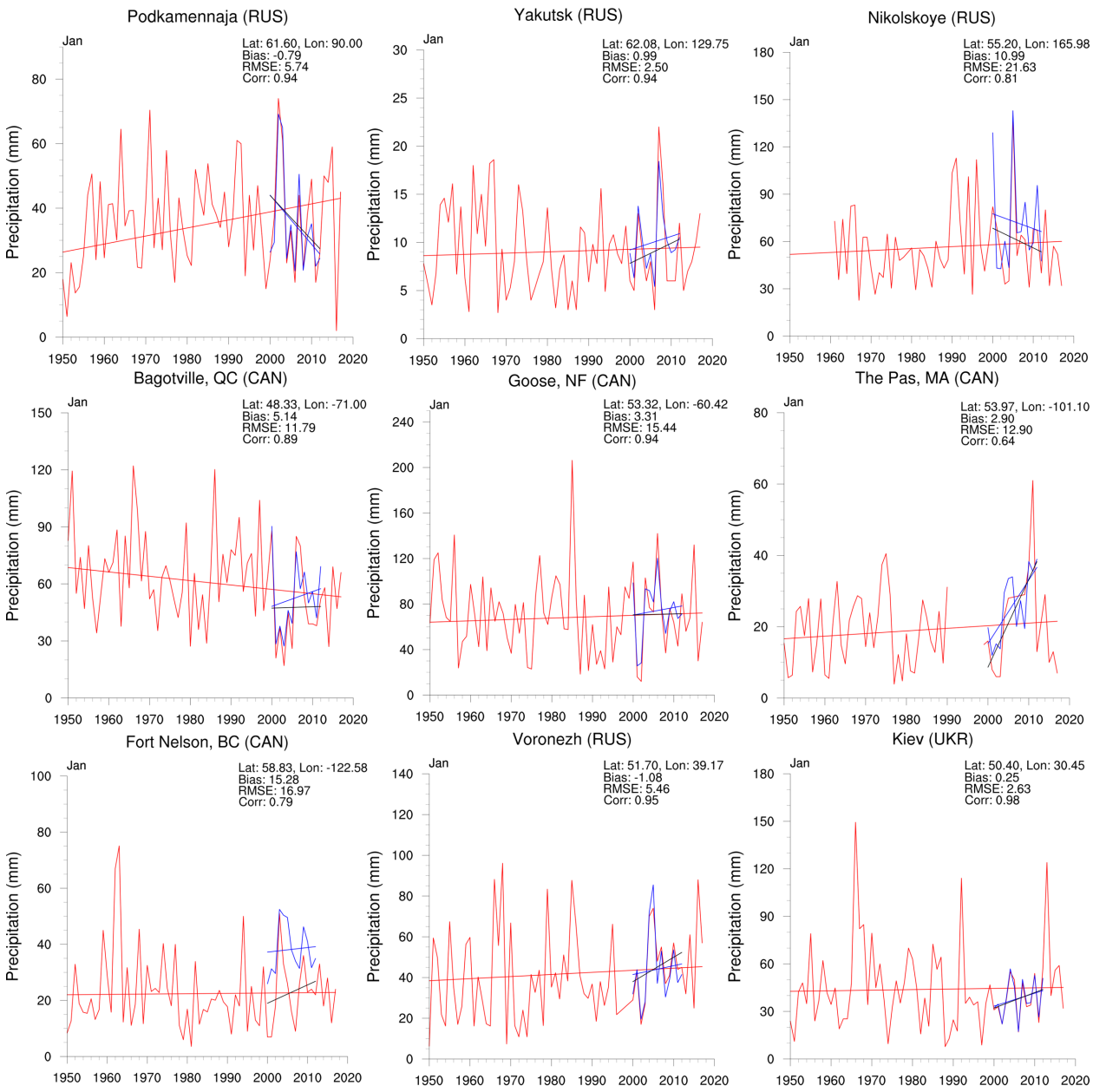

Figure 5: Linear regressions in January total precipitation for nine "validation" stations (records in red), compared to ASR (in blue). A "short term" observation trend was calculated (in black) for in situ records from 2000–2012 for comparison to ASR.

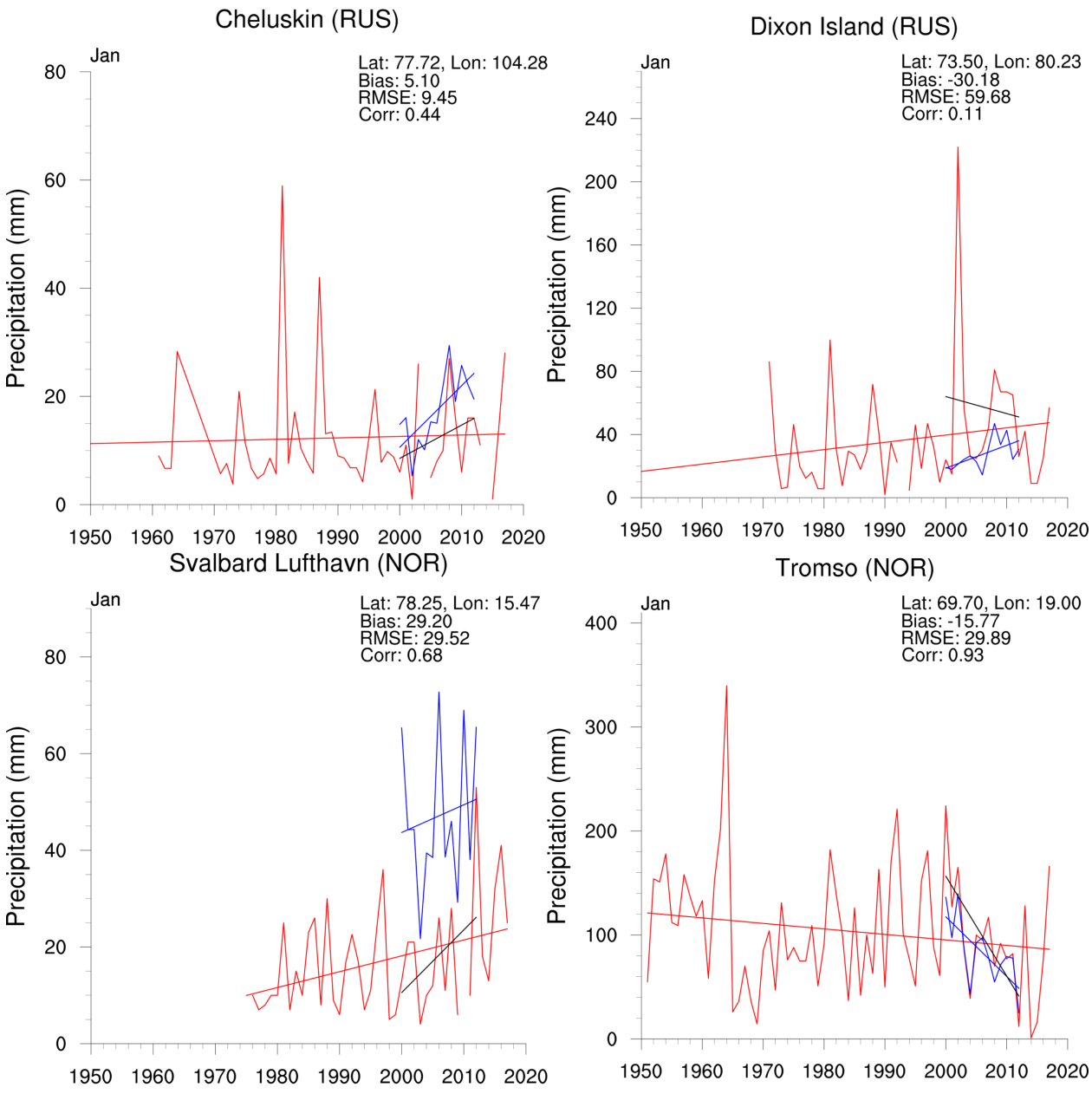

Figure 6: Similar to Figure 5, but for four stations of interest (records in red), compared to ASR (in blue) with a short term observation trend (in black).

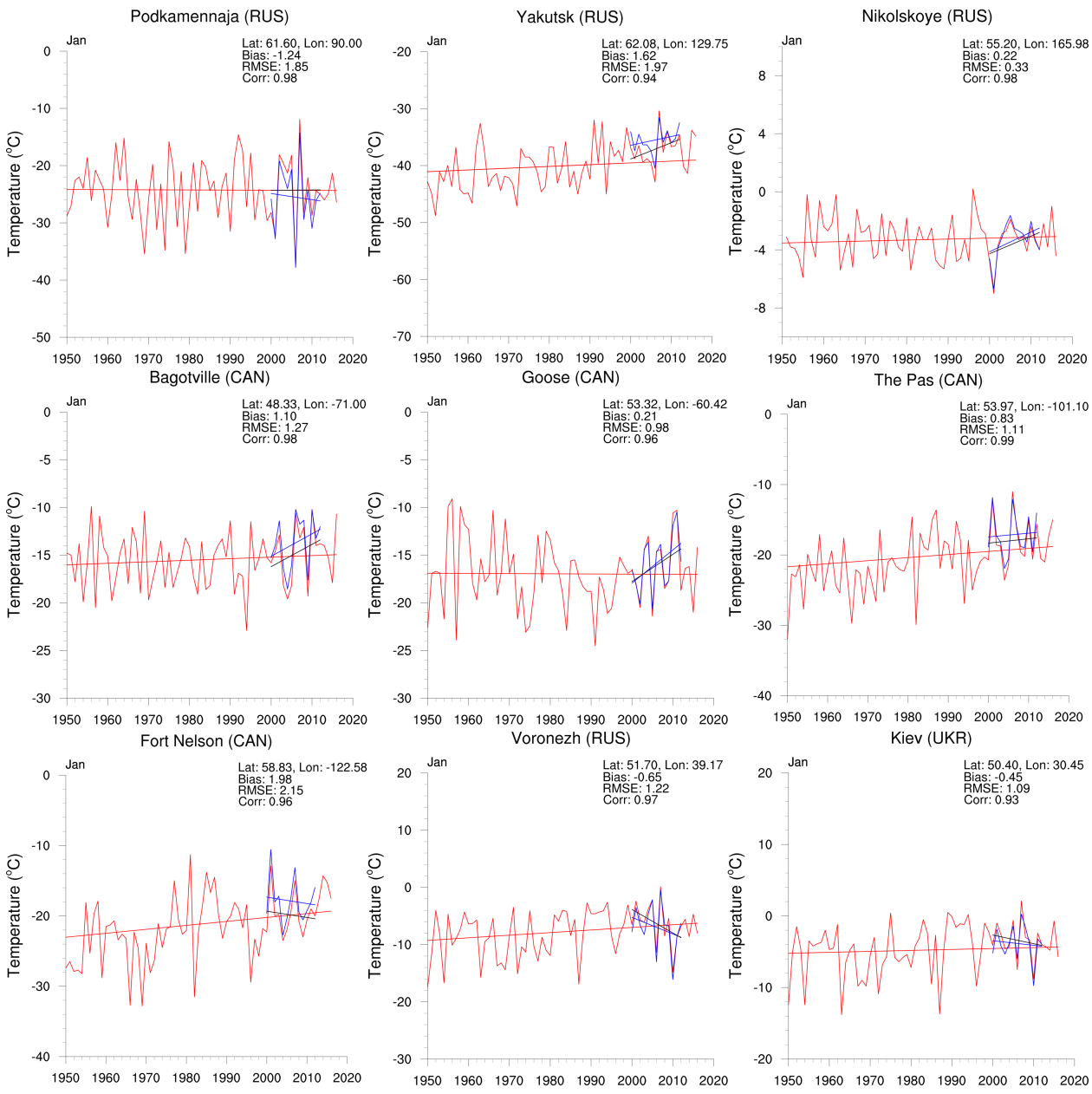

Figure 7: Similar to Figure 5, but for temperature records from nine "validation" stations (records in red), compared to ASR (in blue), with a short term observation trend (in black).

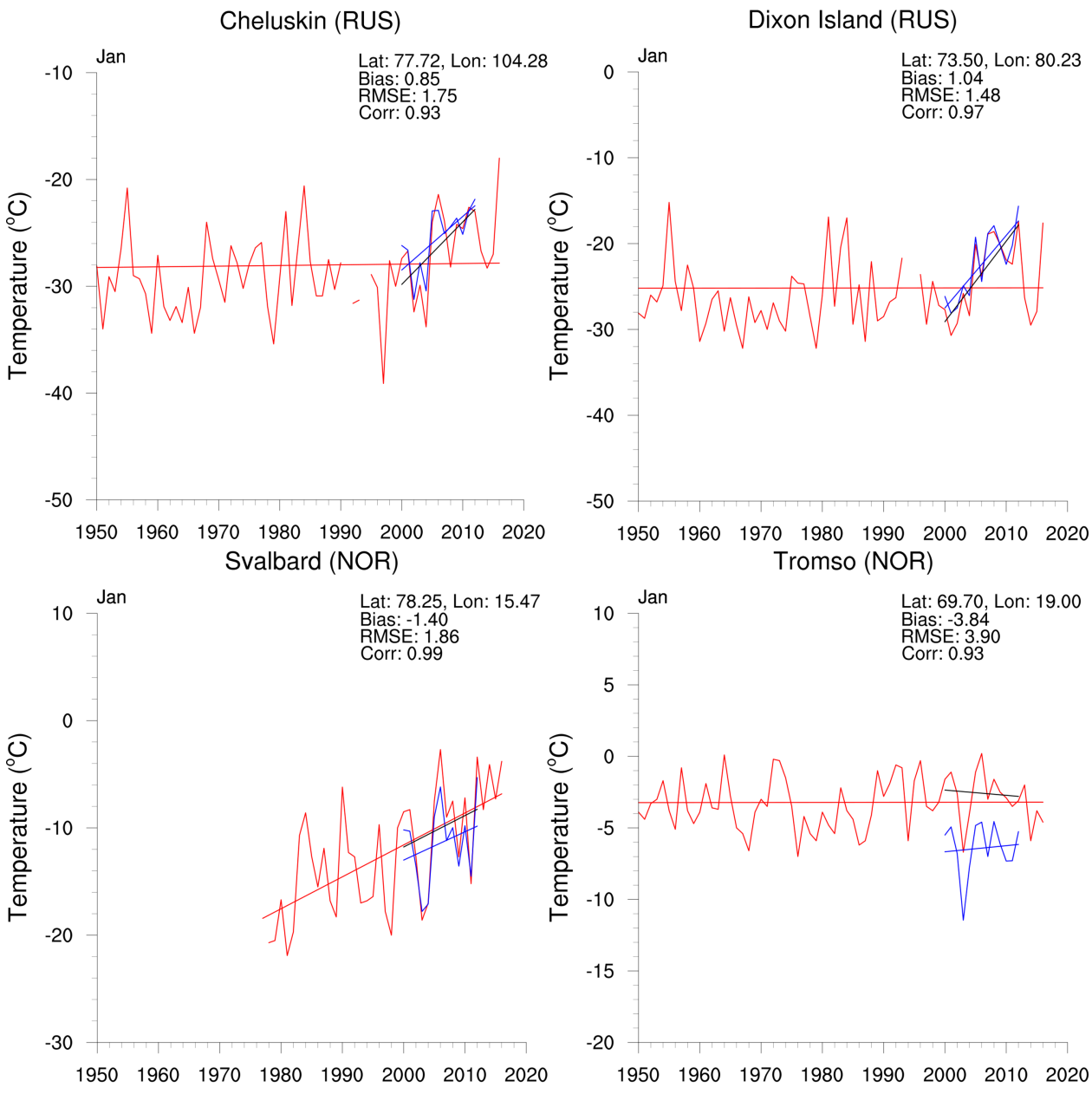

Figure 8: Similar to Figure 6, but for temperature records of four stations of interest (records in red), compared to ASR (in blue) with a short term observation trend (in black).

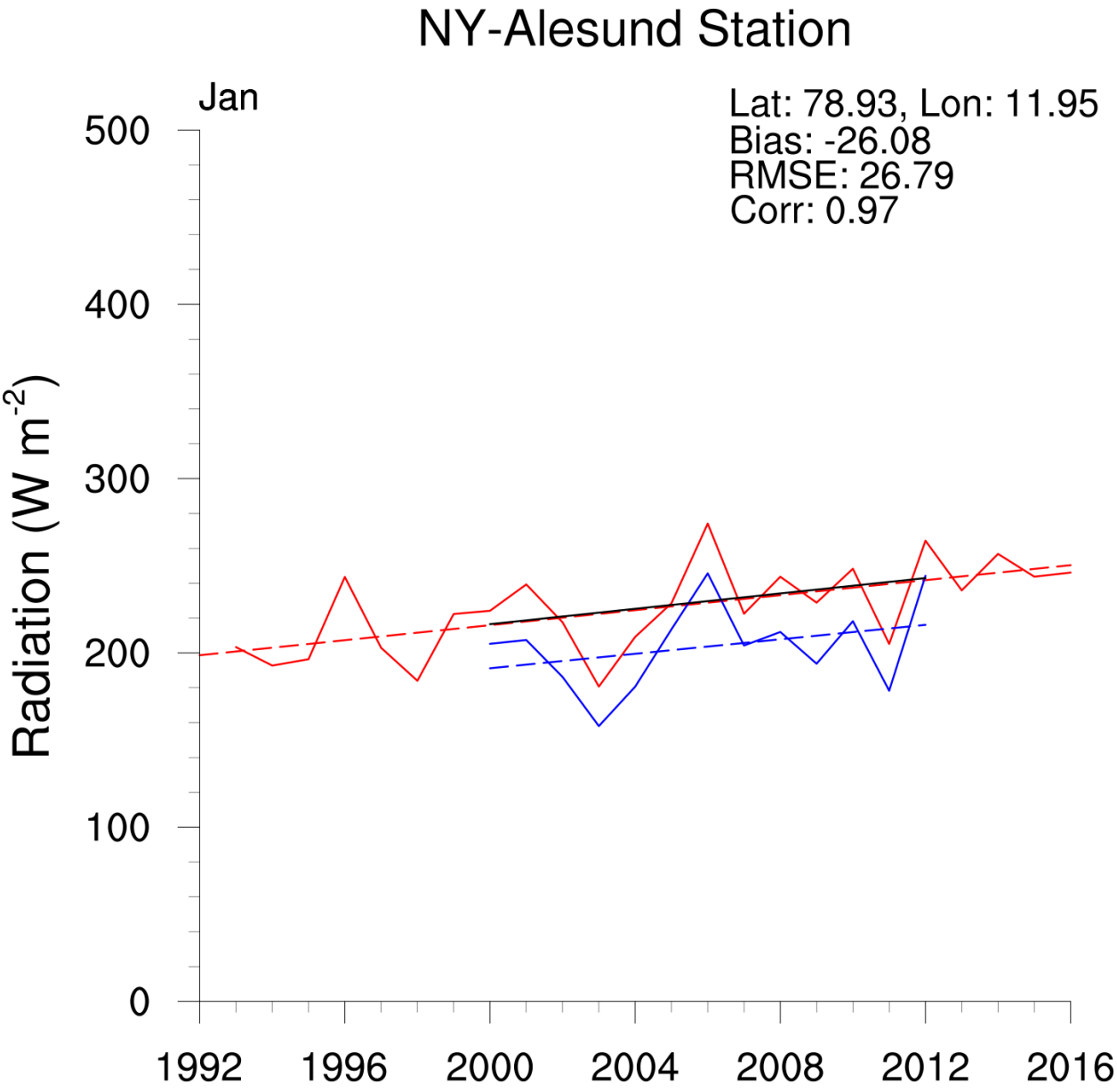

Figure 9: Average January downward longwave radiation (in W m^{-2}) for the Ny-Alesund station. *In situ* measurements (in red) are compared to ASR (in blue).

Station	Latitude	Longitude	Station Description	Bias (mm)	RMSE	Correlation
Podkamennaja (RUS)	61.60 °N	90.00 °E	Airport, flat terrain	-0.79	5.74	0.94
Yakutsk (RUS)	62.08 °N	129.75 °E	Airport, flat terrain	0.99	2.50	0.94
Nikolskoye (RUS)	55.20 °N	165.98 °E	Field, near shore	10.99	21.63	0.81
Bagotville (CAN)	48.33 °N	71.00 °W	Airport, flat terrain	5.14	11.79	0.89
Goose (CAN)	53.32 °N	60.42 °W	Airport, flat terrain	3.31	15.44	0.94
The Pas (CAN)	53.97 °N	101.10 °W	Airport, flat terrain	2.90	12.90	0.64
Fort Nelson (CAN)	58.83 °N	122.58 °W	Airport, flat terrain	15.28	16.97	0.79
Voronezh (RUS)	51.70 °N	39.17 °E	Field, flat terrain	-1.08	5.46	0.95
Kiev (UKR)	50.40 °N	30.45 °E	Airport, flat terrain	0.25	2.63	0.98
Cheluskin (RUS)	77.72 °N	104.28 °E	Varying terrain, near shore	5.10	9.45	0.44
Dixon Island (RUS)	73.50 °N	80.23 °E	Field, near shore	-30.18	59.68	0.11
Svalbard (NOR)	78.25 °N	15.47 °E	Airport, near fjord	29.20	29.52	0.68
Tromsø (NOR)	69.70 °N	19.00 °E	Varying terrain	-15.77	29.89	0.93

Table 1: Summary of statistical comparisons between precipitation records for nine "validation" sites and ASR's interpolation over the time period 2000–2012

Station	Latitude	Longitude	Station Description	Bias (°C)	RMSE	Correlation
Podkamennaja (RUS)	61.60 °N	90.00 °E	Airport, flat terrain	-1.24	1.85	0.98
Yakutsk (RUS)	62.08 °N	129.75 °E	Airport, flat terrain	1.62	1.97	0.94
Nikolskoye (RUS)	55.20 °N	165.98 °E	Field, near shore	0.22	0.33	0.98
Bagotville (CAN)	48.33 °N	71.00 °W	Airport, flat terrain	1.10	1.27	0.98
Goose (CAN)	53.32 °N	60.42 °W	Airport, flat terrain	0.21	0.98	0.96
The Pas (CAN)	53.97 °N	101.10 °W	Airport, flat terrain	0.83	1.11	0.99
Fort Nelson (CAN)	58.83 °N	122.58 °W	Airport, flat terrain	1.98	2.15	0.96
Voronezh (RUS)	51.70 °N	39.17 °E	Field, flat terrain	-0.65	1.22	0.97
Kiev (UKR)	50.40 °N	30.45 °E	Airport, flat terrain	-0.45	1.09	0.93
Cheluskin (RUS)	77.72 °N	104.28 °E	Varying terrain, near shore	0.85	1.75	0.93
Dixon Island (RUS)	73.50 °N	80.23 °E	Field, near shore	1.04	1.48	0.97
Svalbard (NOR)	78.25 °N	15.47 °E	Airport, near fjord	-1.40	1.86	0.99
Tromsø (NOR)	69.70 °N	19.00 °E	Varying terrain	-3.84	3.90	0.93

Table 2: Similar to Table 1 but for temperature records

Station	ASR-interpolated elevation (m)	Station-reported elevation (m)	Difference (m)
Podkamennaja (RUS)	218	60	158
Yakutsk (RUS)	137	98	39
Nikolskoye (RUS)	0	14	-14
Bagotville (CAN)	149	159	-10
Goose (CAN)	190	46	144
The Pas (CAN)	272	271	1
Fort Nelson (CAN)	468	382	86
Voronezh (RUS)	135	147	-12
Kiev (UKR)	107	176	-69
Cheluskin (RUS)	97	13	84
Dixon Island (RUS)	107	42	65
Svalbard (NOR)	247	28	219
Tromsø (NOR)	227	10	217
Ny-Alesund (NOR)	697	11	686

Table 3: Summary of station elevation as reported by station metadata, compared to ASR's interpolation of surface height

REFERENCES CITED

Bromwich, D. H., A. B. Wilson, L. Bai, Z. Liu, M. Barlage, C.-F. Shih, S. B. Maldonado, K. M. Hines, S.-H. Wang, J. Woollen, B. Kuo, H.-C. Lin, T.-K., Wee, M. C. Serreze, and J. E. Walsh, 2017: The Arctic System Reanalysis Version 2. *Bull. Amer. Meteor. Soc.*, accepted

Chaudhuri, A. H. and R.M. Ponte, 2015: An Evaluation of Surface Atmospheric Changes over the Arctic Ocean for 2000–09 Using Recent Reanalyses. *Earth Interactions*, **19**(2), 1-18.

Hassol, S. J., 2005: *Impacts of a Warming Climate: Arctic Climate Impact Assessment*. Cambridge University Press, 139 pp.

Kalnay, E., Kanamitsu, M., Kistler, R., and 19 others, 1996: The NCEP/NCAR 40-Year Reanalysis Project. *Bull. Amer. Meteor. Soc.*, **77**, 437–471.

Kohnemann, S. H. E., G. Heinemann, D. H. Bromwich, and O. Gutjahr, 2017: Extreme warming in the Kara Sea and Barents Sea during the winter period 2000-2016. *J. Clim.*, **30**, 8913-8927, doi: 10.1175/JCLI-D-16-0693.1.

Lindsay, R., M. Wensnahan, A. Schweiger, and J. Zhang, 2014: Evaluation of Seven Different Atmospheric Reanalysis Products in the Arctic. *J. Clim.*, **27**(7), 2588-2606.tfr67cv

Parkinson, C. L., and J. C. Comiso, 2013: On the 2012 Record Low Arctic Sea Ice Cover: Combined Impact of Preconditioning and an August Storm. *Geophys. Res. Lett.*, **40**, 1356–1361, doi:10.1002/grl.50349.

Rothrock, D. A., Y. Yu, and G. A. Maykut, 1999: Thinning of the Arctic sea ice cover. *Geophys. Res. Lett.*, **26**, 3469–3472, doi:10.1029/1999GL010863.

Stroeve, J., M. M. Holland, W. Meier, T. Scambos, and M. Serreze, 2007: Arctic Sea Ice Decline: Faster than Forecast, *Geophys. Res. Lett.*, **34**, L09501, doi:10.1029/2007GL029703

Stroeve, J., M. Serreze, S. Drobot, S. Gearheard, M. Holland, J. Maslanik, W. Meier, and T. Scambos, 2008: Arctic Sea Ice Extent Plummets in 2007. *Eos, Trans.* AGU, **89**(2), 13-14, doi:10.1029/2008EO020001.

APPENDICES

Appendix A: Shell Script for processing BSRN data

```
#!/bin/bash

id="TAT"
st_hgt=25
startmonth=2
startyear=1996
endmonth=2
endyear=2017

i=$startyear
j=$startmonth


while [ $i -le $endyear ]
do
  if [ $i -eq $startyear ]
  then
     while [ $j -le 12 ]
     do
        if [ $j -lt 10 ]
         then
         st_id="zz_${id}_${i}-0${j}_0100+0300"
        else
         st_id="zz_${id}_${i}-${j}_0100+0300"
        fi
     ncl -Qn bsrn_edit.ncl 'stid="'${st_id}'"' 'sthgt="'${st_hgt}'"'
     true $(( j++ ))
     done
  true $(( i++ ))
  j=1

  elif [ $i -gt $startyear -a $i -lt $endyear ]
  then
     while [ $j -le 12 ]
  do
     if [ $j -lt 10 ]
     then
         st_id="zz_${id}_${i}-0${j}_0100+0300"
        else
         st_id="zz_${id}_${i}-${j}_0100+0300"
     fi
  ncl -Qn bsrn_edit.ncl 'stid="'${st_id}'"' 'sthgt="'${st_hgt}'"'
  true $(( j++ ))
  done
  true $(( i++ ))
  j=1

  elif [ $i -eq $endyear ]
  then
     while [ $j -le $endmonth ]
  do
     if [ $j -lt 10 ]
     then
         st_id="zz_${id}_${i}-0${j}_0100+0300"
        else
         st_id="zz_${id}_${i}-${j}_0100+0300"
     fi
  ncl -Qn bsrn_edit.ncl 'stid="'${st_id}'"' 'sthgt="'${st_hgt}'"'
  true $(( j++ ))
  done
  true $(( i++ ))
  j=1

  fi
done
exit
```

Appendix B: NCL Script for processing BSRN data from text files to netCDF files

```
load "$NCARG_ROOT/lib/ncarg/nclscripts/csm/contributed.ncl"
begin

path_id  = "tat"
st_title = "Tateno"

datapath = "/txt_files/"
data = rm_single_dims(readAsciiTable(datapath+stid+".txt",1,"string",1))
data@_FillValue   = -999
nl = dimsizes(data)

dmap = (/4,1,2,1,2,1,2,1,7,20,20,20,20,20,20,20,20,20,20,20/)
dbreak = str_split_by_length(data,dmap)
print(stid+ "       " +dimsizes(dbreak(1,:)))

yy = toint(dbreak(:,0))
mm = toint(dbreak(:,2))
dd = toint(dbreak(:,4))
hh = toint(dbreak(:,6))
mn = toint(dbreak(:,8))
ss = mn
ss = 0


xdata = new((/11,nl/),float)
xdata = -999.
xdata@_FillValue   = -999.
xdata!1 = "time"
xdata(0,:) = tofloat(dbreak(:, 9))  ; lat
xdata(1,:) = tofloat(dbreak(:,10))  ; lon
xdata(2,:) = tofloat(dbreak(:,11))  ; sw (global) down
xdata(3,:) = tofloat(dbreak(:,12))  ; lw down

ndim = dimsizes(dbreak)
if (ndim(1).eq.15) then
  xdata(4,:) = tofloat(dbreak(:,13))  ; sw up
  xdata(5,:) = tofloat(dbreak(:,14))  ; lw up
else if (ndim(1).eq.17) then
  xdata( 6,:) = tofloat(dbreak(:,15)) ; air temp (C)
  xdata( 7,:) = tofloat(dbreak(:,16)) ; relative humidity (%)
else if (ndim(1).eq.18) then
  xdata( 6,:) = tofloat(dbreak(:,15)) ; air temp (C)
  xdata( 7,:) = tofloat(dbreak(:,16)) ; relative humidity (%)
  xdata( 8,:) = tofloat(dbreak(:,17)) ; station pressure (hPa)
```

```
end if
end if
end if

units= "minutes since 1990-01-01 00:00:00"

opt=0
opt@return_type = "float"
t1=cd_inv_calendar(yy,mm,dd,hh,mn,ss,units,opt)
tt=round(t1,3)


sw_dwn  = t1
sw_dwn = xdata(2,:)
sw_dwn@description = "Short-Wave downward (global) [W/m2]"
sw_dwn!0 = "time"
sw_dwn&time = tt

lw_dwn  = t1
lw_dwn = xdata(3,:)
lw_dwn@description = "Longwave downward radiation [W/m2]"
lw_dwn!0 = "time"
lw_dwn&time = tt

sw_up = t1
sw_up = xdata(4,:)
sw_up@description = "Shortwave upward radiation [W/m2]"
sw_up!0 = "time"
sw_up&time = tt

lw_up = t1
lw_up = xdata(5,:)
lw_up@description = "Longwave upward radiation [W/m2]"
lw_up!0 = "time"
lw_up&time = tt

temp = t1
temp = xdata(6,:)
temp@description = "Air temp [C]"
temp!0 = "time"
temp&time = tt

relH = t1
relH = xdata(7,:)
relH@description = "Relative Humidity [%]"
relH!0 = "time"
```

```
relH&time = tt

pres = t1
pres = xdata(8,:)
pres@description = "Station Pressure [hPa]"
pres!0 = "time"
pres&time =tt


globalAtt           = True
globalAtt@Title     = st_title + " Station"
globalAtt@latitude  = xdata(0,0)
globalAtt@longitude = xdata(1,0)
globalAtt@height    = sthgt
globalAtt@units     = "minutes since 1990-01-01 00:00:00"
globalAtt@calendar  = "standard"


dir="/export/nc_files/"
fo=dir+stid+".nc"

system(("/bin/rm -f "+fo))
ncdf = addfile(fo,"c")
fileattdef( ncdf, globalAtt )
filedimdef(ncdf,"time",-1,True)

ncdf->SW_DWN   = sw_dwn
ncdf->LW_DWN   = lw_dwn
ncdf->SW_UP    = sw_up
ncdf->LW_UP    = lw_up
ncdf->TEMP     = temp
ncdf->RELH     = relH
ncdf->PRES     = pres



end
```

Appendix C: NCL Script for averaging BSRN data at 3 hour (+/- 30 minutes) intervals

```
load "$NCARG_ROOT/lib/ncarg/nclscripts/csm/contributed.ncl"
begin

dir =systemfunc ("ls /nc_files/pay/*")
a = addfiles(dir,"r")
b = addfile("/nc_files/pay/PAY_2004-08.nc","r")

sw_down = a[:]->SW_DWN
sw_up   = a[:]->SW_UP
lw_down = a[:]->LW_DWN
lw_up   = a[:]->LW_UP
temp    = a[:]->TEMP
humid   = a[:]->RELH
pres    = a[:]->PRES

delete(a)

time = pres
time = pres&time
time@_FillValue = -999

step = 180   ; three hour time steps
array=new((/7,round(((time(dimsizes(time)-1)-time(0))/step),3)/),float)
array!1 = "time"
array@_FillValue = -999

dummytime = new((/round(((time(dimsizes(time)-1)-time(0))/step),3)/),"integer")

tcount = round(time(0),3)
tcount@units = time@units

icount = 0

do while tcount.lt.time(dimsizes(time)-1)

  aa:=ind(sw_down&time.gt.(tcount-30).and.sw_down&time.lt.(tcount+30))
  dummytime(icount)=tcount
  if .not.ismissing(min(aa)) then
    array(0,icount)=avg(sw_down(ind(sw_down&time.gt.(tcount-
30).and.sw_down&time.lt.(tcount+30))))
    array(1,icount)=avg(lw_down(ind(lw_down&time.gt.(tcount-
30).and.lw_down&time.lt.(tcount+30))))
    array(2,icount)=avg(sw_up(ind(sw_up&time.gt.(tcount-30).and.sw_up&time.lt.(tcount+30))))
    array(3,icount)=avg(lw_up(ind(lw_up&time.gt.(tcount-30).and.lw_up&time.lt.(tcount+30))))
    array(4,icount)=avg(temp(ind(temp&time.gt.(tcount-30).and.temp&time.lt.(tcount+30))))
    array(5,icount)=avg(humid(ind(humid&time.gt.(tcount-30).and.humid&time.lt.(tcount+30))))
```

```
    array(6,icount)=avg(pres(ind(pres&time.gt.(tcount-30).and.pres&time.lt.(tcount+30))))
  else
    array(:,icount)=array@_FillValue
  end if

  print(cd_calendar(tcount,0))
  print(array(0,icount))
  tcount = tcount+step
  icount = icount+1

end do

array&time = dummytime
array@units = time@units

dr="/post_avg/"
fo=dr+"pay_3hour_avg.nc"

system(("/bin/rm -f "+fo))
ncdf = addfile(fo,"c")
filedimdef(ncdf,"time",-1,True)


global_attnames = getvaratts(b)
do i=0,dimsizes(global_attnames)-1
ncdf@$global_attnames(i)$ = b@$global_attnames(i)$
end do

ncdf->SW_DWN   = array(0,:)
ncdf->LW_DWN   = array(1,:)
ncdf->SW_UP    = array(2,:)
ncdf->LW_UP    = array(3,:)
ncdf->TEMP     = array(4,:)
ncdf->RELH     = array(5,:)
ncdf->PRES     = array(6,:)

end
```

Appendix D: NCL Script for processing GHCN files to netCDF files

```
load "$NCARG_ROOT/lib/ncarg/nclscripts/csm/contributed.ncl"
begin

datapath = “/stations/temp_/"
data = readAsciiTable(datapath+stid+".csv",13, "float",0)

data@_FillValue   = -999
data1=data(:,1:12)
data1=data1/100.


yyyy = data(:,0)
nl = dimsizes(yyyy)
units= "hours since 1900-01-01 00:00:00"


junkyear   = new((nl*12),float)
junkmonth  = junkyear
junkday    = junkyear
junkhr     = junkyear
junkmin    = junkyear
junksec    = junkyear
junkday    = 1
junkhr     = 0
junkmin    = 0
junksec    = 0

i=0
do while(i.le.dimsizes(junkyear)-1)
     junkyear(i)  = yyyy(toint(floor(i/12)))
     junkmonth(i) = mod(i,12)+1
     i=i+1
end do
t1=cd_inv_calendar(junkyear,junkmonth,junkday,junkhr,junkmin,junksec,units,0)
newprecip=reshape(data1,nl*12)

newprecip@_FillValue   = -999
newprecip@station_name = stname
newprecip@station_code = stid
newprecip@lat         = stlat
newprecip@lon         = stlon
newprecip@hgt         = sthgt
```

```
xdate=t1
xdate@units = "hours since 1900-01-01 00:00:00"
xdate@calendar = "standard"
xdate!0 = "time"
newprecip!0 = "time"
xdate&time = xdate
newprecip&time = xdate

dir="/temp_/nc_files/"
fo=dir+stid+".nc"
print(fo)

system(("/bin/rm -f"+ fo))
ncdf = addfile(fo,"c")
filedimdef(ncdf,"time",-1,True)
ncdf->TEMP    = newprecip
end
```

Appendix E: NCL Script for interpolating GHCN data and comparing to ASR

```
load "$NCARG_ROOT/lib/ncarg/nclscripts/csm/contributed.ncl"
begin

stid = "222_32618_000"
mm   = "01"
mo=toint(mm)

;load lat/lon data
a = addfile("/ASR-v2/invariant/asr15km.fix.2000010100.XLAT.nc","r")
b = addfile("/ASR-v2/invariant/asr15km.fix.2000010100.XLONG.nc","r")

lat2d = a->XLAT(:,:)
lon2d = b->XLONG(:,:)

;load ASR data
dir =systemfunc ("ls /ASR-v2/forecast/sfc/asr15km.fct.2D*")
c = addfiles(dir,"r")
;rainc  = c[:]->RAINC
;rainnc = c[:]->RAINNC
;precipraw = rainc+rainnc

precipraw = c[:]->T2M
precipraw = precipraw - 273.15

precip = reshape(precipraw,(/13,12,720,720/))

;do i = 0,11
;     precip(:,i,:,:)=precip(:,i,:,:)*days_in_month(2000,i+1)*8
;end do

delete([/a,b,c/])

dr = "/stations/temp_/nc_files/"
d = addfile(dr+stid+".nc","r")
;ghcn_data = d->PRCP

ghcn_data = d->TEMP
ghcn_name = ghcn_data@station_name
ghcn_code = ghcn_data@station_code
ghcn_lat  = stringtofloat(ghcn_data@lat)
ghcn_lon  = stringtofloat(ghcn_data@lon)
ghcn_hgt  = stringtofloat(ghcn_data@hgt)
```

```
ASR_interp     = rm_single_dims(rcm2points(lat2d,lon2d,precip(:,mo-1,:,:),ghcn_lat,ghcn_lon,2))
ASR_tline      = ASR_interp
ASR_yr         = ispan(2000,2012,1)

ASR_rc         = regline_stats(ASR_yr,ASR_interp)
ASR_tline      = ASR_rc*(ASR_yr)+ASR_rc@yintercept
ASR_pv         = ASR_rc@pval

ASR_plot       = new((/2,dimsizes(ASR_interp)/), typeof(ASR_interp))
ASR_plot(0,:)    = ASR_interp
ASR_plot(1,:)    = ASR_tline

ghcn_time = cd_calendar(ghcn_data&time,-5)
ghcn_mo   = ghcn_time(:,1)
imm = ind(ghcn_mo.eq.mo)
ghcn_year = ghcn_time(imm,0)

ghcn_rc       = regline_stats(ghcn_year,ghcn_data(imm))
ghcn_tline    = ghcn_rc*(ghcn_year)+ghcn_rc@yintercept
ghcn_pv       = ghcn_rc@pval

ghcn_sub=ghcn_data(imm)
ghcn_sub_yr = ghcn_year(ind(ghcn_year.ge.ASR_yr(0).and.ghcn_year.le.ASR_yr(12)))
ghcn_ASR_rc  =
regline_stats(ghcn_sub_yr,ghcn_sub(ind(ghcn_year.ge.ASR_yr(0).and.ghcn_year.le.ASR_yr(12))))
ghcn_ASR_tl   = ghcn_ASR_rc*(ASR_yr)+ghcn_ASR_rc@yintercept
ghcn_ASR_pv   = ghcn_ASR_rc@pval

ghcn_plot     = new((/2,dimsizes(ghcn_data(imm))/), typeof(ghcn_data))
ghcn_plot(0,:)  = ghcn_data(imm)
ghcn_plot(1,:)  = (/ghcn_tline/)



ASR_junk_years = (get1Dindex(ASR_yr,ghcn_sub_yr))

station_junk = ghcn_sub(ind(ghcn_year.ge.ASR_yr(0).and.ghcn_year.le.ASR_yr(12)))

rmse = dim_rmsd(ASR_interp(ASR_junk_years),station_junk)
corr = escorc(ASR_interp(ASR_junk_years),station_junk)
aaaa = avg(ASR_interp(ASR_junk_years))
bbbb = avg(station_junk)
bias = (aaaa-bbbb)

month_abbr = (/"","Jan","Feb","Mar","Apr","May","Jun","Jul","Aug","Sep", \
                    "Oct","Nov","Dec"/)

max_data = max( (/max(ghcn_data(imm)),max(ASR_interp)/) )  ; mod by wsh
```

```
min_data = min( (/min(ghcn_data(imm)),min(ASR_interp)/) )
;print(max_data + "  "+min_data)

ghcn_max = (ceil(.12*max_data))*10
ghcn_min = (floor(.12*min_data))*10
;ghcn_max = 20
;ghcn_min = -20


;;;;;;;;;;;;;; Plot Time Series;;;;;;;;;;;;;;;;;;;;;;;;;;;;;;;;;;;;;;;;;;

plDir = "/Output/new_temp/"
plFile= stid+"_m"+mm

wks_type = "png"
wks_type@wkWidth  = 1500
wks_type@wkHeight = 1500

wks   = gsn_open_wks(wks_type,plDir+plFile)
;;;;;;;;;;;;;;;;;;;;;;;;;;;;;;;;;;;;;;;;;;;;;;;;;;;;;;;;;;;;;;;;;;;;;;;;;;;

res                     = True
res@gsnMaximize         = True
res@gsnDraw             = False
res@gsnFrame            = False
res@xyMarkerColor       = "red"                    ; Marker color
res@xyLineColor         = (/"red","red"/)          ; Line color
res@xyLineThicknessF    = 5.0
res@trYMinF             = ghcn_min
res@trYMaxF             = ghcn_max
res@tmYROn              = False
res@trXMinF             = 1950
res@trXMaxF             = 2020
res@tmXTOn              = False
res@tmYRBorderOn        = False
res@tmXTBorderOn        = False
res@tiMainString        = ghcn_name
res@gsnLeftString       = month_abbr(mo)
res@tiYAxisString       = "Temperature (~S~o~N~C)"
res@xyDashPattern       = (/0, 0/)

;;;;;;;;;;;;;;;;;;;;;;;;;;;;;;;;;;;;;;;;;;;;;;;;;;;;;;;;;;;;;;;;;;;;;;;;;;;

txres               = True                     ; text mods desired
txres@txFontHeightF = 0.024                   ; text font height
txres@txJust        = "CenterLeft"             ; Default is "CenterCenter".
```

```
plot  = gsn_csm_xy(wks,ghcn_year,ghcn_plot,res)

res@xyLineColor      = (/"blue","blue"/)
res@xyMarkerColor    = "blue"
overlay(plot,gsn_csm_xy(wks,ASR_yr,ASR_plot,res))

res@xyLineColor       = (/"black","black"/)
res@xyMarkerColor     = "black"
overlay(plot,gsn_csm_xy(wks,ASR_yr,ghcn_ASR_tl,res))
gsn_text_ndc(wks,sprintf("Lat: %4.2f",ghcn_lat)+sprintf(", Lon: %4.2f",ghcn_lon),0.65,0.88,txres)
gsn_text_ndc(wks,sprintf("Bias: %4.2f",bias),0.65,0.85,txres)
gsn_text_ndc(wks,sprintf("RMSE: %4.2f",rmse),0.65,0.82,txres)
gsn_text_ndc(wks,sprintf("Corr: %4.2f",corr),0.65,0.79,txres)

draw(plot)
frame(wks)

end
```